Journal of Power Sources 190 (2009) 279–284

Contents lists available at ScienceDirect

Journal of Power Sources

journal homepage: www.elsevier.com/locate/jpowsour

Low methanol-permeable polyaniline/Nafion composite membrane for direct methanol fuel cells

C.-H. Wang[a,b], C.-C. Chen[c], H.-C. Hsu[d], H.-Y. Du[d], C.-P. Chen[d], J.-Y. Hwang[d], L.C. Chen[d,**], H.-C. Shih[b], J. Stejskal[e], K.H. Chen[a,d,*]

[a] Institute of Atomic and Molecular Sciences, Academia Sinica, Taipei 10617, Taiwan
[b] Department of Materials Science and Engineering, National Tsing Hua University, Hsinchu 30013, Taiwan
[c] Department of Chemistry, National Taiwan Normal University, Taipei 11677, Taiwan
[d] Center for Condensed Matter Sciences, National Taiwan University, Taipei 10617, Taiwan
[e] Institute of Macromolecular Chemistry, Academy of Sciences of the Czech Republic, 162 06 Prague 6, Czech Republic

ARTICLE INFO

Article history:
Received 28 October 2008
Received in revised form 30 December 2008
Accepted 30 December 2008
Available online 14 January 2009

Keywords:
DMFC
Methanol crossover
Polyaniline
Nafion

ABSTRACT

Protonated polyaniline (PANI) is directly polymerized on Nafion 117 (N117), forming a composite membrane, to act as a methanol-blocking layer to reduce the methanol crossover in the direct methanol fuel cell (DMFC), which is beneficial for the DMFC operating at high methanol concentration. The PANI layer grown on the N117 with a thickness of 100 nm has an electrical conductivity of 13.2 S cm^{-1}. The methanol permeability of the PANI/N117 membrane is reduced to 59% of that of the N117 alone, suggesting that the PANI/N117 can effectively reduce the methanol crossover in the DMFC. Comparison of membrane-electrode-assemblies (MEA) using the conventional N117 and the newly developed PANI/N117 composite shows that the PANI/N117-based MEA outputs higher power at high methanol concentration, while the output power of the N117-based MEA is reduced at high methanol concentration due to the methanol crossover. The maximum power density of the PANI/N117-based MEA at 60 °C is 70 mW cm^{-2} at 6 M methanol solution, which is double the N117-based MEA at the same methanol concentration. The resistance of PANI/N117 composite membrane is reduced at elevated methanol concentration, due to the hydrogen bonding between methanol and PANI pushes the polymer chains apart. It is concluded that the PANI/N117-based MEA performs well at elevated methanol concentration, which is suitable for the long-term operation of the DMFC.

1. Introduction

Direct methanol fuel cell (DMFC) is an electrochemical power source utilizing methanol solution and air/oxygen at the anode and the cathode, respectively. The DMFC with the advantages of low temperature operation, ease of fuel storage and a simple design that requires no reformer is regarded as a promising power source for portable applications [1–4]. As shown in Table 1, a high methanol concentration, namely, high specific energy density is a basic requirement in the fabrication of the small-scale DMFC for long-term operation.

The Nafion (DuPont) membrane, which is widely used in a proton exchange membrane (PEM)-based fuel cell, is a good proton-conducting membrane to connect the anode and cathode. However, it is highly permeable for methanol through the water-filled pores in the membrane [5,6], resulting in low fuel efficiency and reduced cathode activity due to the mixed potential effect and the mass-transfer effect at the cathode. Accordingly, a new proton-conducting membrane with low methanol permeability is essential to the development of DMFCs. Many approaches have been proposed to design low methanol-permeable membrane materials, including the modification of Nafion [7–10], the alternative proton-conducting membranes [11–13], and composite proton-conducting membranes [12–15]. However, most of them suffer from major drawbacks such as low proton conductivity, poor mechanical strength, and inferior chemical and thermal stability at elevated temperatures [16].

Preparation of a thin methanol-blocking layer on the Nafion is a direct approach for a stable and mechanically strong composite membrane with low methanol permeability while maintaining high proton conductivity. Protonated polyaniline (PANI), which has an electrical conductivity of 1–10 S cm^{-1}, can act as an electrical conductor to improve the performance of DMFC. Its electrochemical stability makes it even more attractive for the corrosive environment in fuel cells [17–20]. Some efforts have been

* Corresponding author at: Institute of Atomic and Molecular Science, Academia Sinica, Taipei 10617, Taiwan.
** Co-corresponding author.
E-mail addresses: chenlc@ntu.edu.tw (L.C. Chen), chenkh@pub.iams.sinica.edu.tw (K.H. Chen).

0378-7753/$ – see front matter © 2009 Elsevier B.V. All rights reserved.
doi:10.1016/j.jpowsour.2008.12.125

Table 1
The methanol concentrations with respect to their energy properties in the DMFC.

Methanol molarity (M)	1	2	4	6	8	10	Pure
Methanol (wt.%)	3.22	6.47	13.20	19.90	26.81	33.86	100.00
Energy density (Wh g^{-1})	0.196	0.394	0.803	1.21	1.63	2.06	6.08
Ratio of energy density of specific molarity to that of 1 M	1.00	2.01	4.10	6.17	8.32	10.51	31.02
Theoretical feeding rate of fuel to generate 1 W (mg min^{-1})[a]	85.03	42.30	20.76	13.77	10.22	8.09	2.74

[a] The cell potential is assumed as 1.2 V.

made in utilizing PANI composite membrane, e.g., PANI/Nafion, PANI/PEEK, PANI/SPEEK and PANI/Silica/Nafion, as the methanol-blocking layer for DMFCs [20–26]. Choi et al. [24] and Huang et al. [25] presented that the PANI/Nafion composite membrane had lower methanol permeability and performed higher membrane-electrode-assemblies (MEA) performance by feeding 2 M methanol compared to Nafion membrane. However, they also pointed out that the PANI/Nafion composite membrane has lower proton conductivity than Nafion membrane, which limited PANI/Nafion performance operating at high methanol concentration.

In this work, the performance of a low methanol-permeable PANI/Nafion composite membrane for DMFC operated at elevated methanol concentration has been investigated. Protonated PANI was directly polymerized on the Nafion 117 (N117) membrane to form a PANI/N117 composite membrane. The specific membrane and Pt-based electrodes were hot-pressed to form the MEA. Various performance tests including polarization curves at different methanol concentrations and the methanol-crossover rate have been carried out on the PANI/117-based MEA. Various performance tests including polarization curves at different methanol concentrations and the methanol-crossover rate have been carried out on the PANI/117-based MEA, showing that PANI/N117 composite membrane is suitable to operate at high methanol concentration.

2. Experimental

The technique reported by Stejskal and Gilbert [27] for the synthesis of the protonated PANI is adopted in this study. The PANI preparation was performed by mixing aniline hydrochloride with ammonium persulfate to yield PANI at the ambient temperature (Fig. 1). A stoichiometric persulfate/aniline ratio of 1.25 has been used [27–29] to minimize the amount of residual aniline and to optimize the yield of PANI. Aniline hydrochloride (1.295 g) was dissolved in 2 M hydrochloric acid solution containing 4 wt.% polyvinylpyrrolidone (PVP; type K-30, Fluka) to give 50 ml of the solution. According to the work of Stejskal and Gilbert, adding hydrochloric acid to the process will increase the conductivity of PANI [27]. The added PVP acts not only as a stabilizer but also as an accelerator for the polymerization [30–32], and improves the quality of deposited PANI film [31]. Ammonium persulfate (2.855 g) was dissolved in water to yield 50 ml of the solution. When the aniline hydrochloride and the ammonium persulfate solutions were mixed for polymerization, the N117 was rapidly immersed in the mixture for 30 min. In this approach only one side of the N117 is coated with PANI while the other side is secluded by an adhesive tape during the polymerization. In this way, the PANI/N117 composite can reduce methanol permeability without undermining the electron and proton conduction. Following the PANI polymerization, the PANI/N117 was removed from the mixture, and was then washed in 0.2 M HCl before being rinsed in acetone to remove residual monomers, oxidants, low-molecular-weight organic intermediates and oligomers [27].

Two square gold electrodes (each of 1.5×10^{-4} m long and 1×10^{-5} m thick) were coated on an undoped silicon substrate at a distance of 1×10^{-7} m to measure the electrical conductivity of the PANI layer. The dual-electrodes were immersed in the reaction mixtures for the polymerization of the PANI layer between the electrodes followed by conductivity measurement using a Keithley-4200 multi-functional electrometer. The morphology of the PANI/N117 was studied using a high-resolution scanning electron microscopy (HRSEM, JEOL-6700), and the film thickness was directly estimated from the cross-sectional HRSEM image. The surface roughness of the PANI/N117 was determined by atomic force microscopy in tapping mode (AFM, JPK nanowizard). In order to measure the proton conductivity of the membrane, it was placed in between two gold plates and followed by ac impedance measurement (Solartron 1280Z spectrometer) at the frequency range from 20 kHz to 0.1 Hz, in a humidity of 100% throughout the measurement. The methanol permeability was determined from the flux of the methanol crossover of the membrane with the PANI/Nafion membrane placed in between a 2 M aqueous methanol solution and a de-ionized water. The methanol concentrations in the two solutions were measured using gas chromatography (GC 9800, China Chromatography Co.) to determine the permeability.

In the preparation of the MEAs, electrodes of a 80 wt.% 4.0 mg cm^{-2}-Pt–Ru on carbon cloth and a 5.0 mg cm^{-2}-Pt black on carbon cloth were used as the anode and cathode, respectively. They underwent the same hot-pressed condition at 130 °C and 130 kg cm^{-2} for 2 min. Fig. 2a and b present the schematic structures of the N117-based MEA and PANI/N117-based MEA, respectively, in which a PANI layer is sandwiched between the N117 and the anodic catalyst layer with PANI facing the anode. In the polarization curve measurement, methanol solutions of various concentrations were pumped into the anode chamber at a rate of 20 ml cm^{-3} and the oxygen flowed into the cathode chamber at a rate of 200 sccm. The cell temperature was maintained at 60 °C during all the measurements.

Electrochemical technique was employed in the fuel cell to determine the methanol-crossover rate of the MEA [33,34]. The nitrogen flowed into the cathode at a rate of 200 sccm, and a positive voltage was applied to the cathode using a potentiostat (SI 1280Z, Solartron). Therefore, the methanol at the cathode was oxidized to CO_2 under the applied voltage. When the applied voltage was high enough to oxidize all methanol molecules quickly at the cathode, the methanol-crossover limiting current was reached.

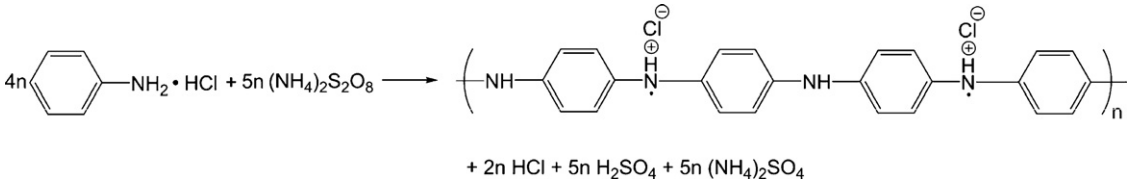

Fig. 1. Oxidation of aniline hydrochloride with ammonium persulfate yielding polyaniline (PANI).

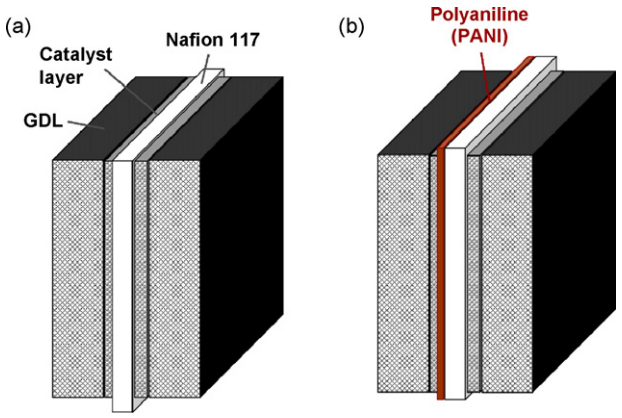

Fig. 2. The prepared structures of (a) the N117-based MEA and (b) the PANI/N117-based MEA.

The methanol-crossover limiting current was associated with the methanol-crossover rate at the open circuit [33,34], and is given by the following equation,

$$j_{\text{xover}} = nF \times v_{\text{xover}}, \tag{1}$$

where j_{xover} denotes the methanol-crossover limiting current density; n is the number of electrons that are involved in the oxidation of methanol, F is the Faraday constant, and v_{xover} is the methanol-crossover rate. The v_{xover} can be expressed as,

$$v_{\text{xover}} = -D_{\text{M}} \frac{\partial C_{\text{M}}}{\partial x_{\text{m}}}, \tag{2}$$

where D_{M} and $\partial C_{\text{M}}/\partial x_{\text{m}}$ are the methanol permeability constant and the methanol concentration gradient through the thickness of the membrane, respectively.

3. Results and discussion

Fig. 3a shows the cross-sectional HRSEM image of a PANI layer coated on the silicon substrate, indicating a 30 nm thickness of a PANI layer. Fig. 3b shows the cross-sectional HRSEM image of a PANI layer on the N117 with a PANI thickness of about 100 nm. The PANI is preferentially coated on the N117 during polymerization, which is in agreement with the results of Barthet and Guglielmi [35,36]. It indicates that the PANI was compatible with the Nafion perhaps because of the formation of ionic bonds between the sulfonated acid of the N117 and the imine groups of the PANI. Fig. 3c depicts the AFM profile of the PANI/N117 in the 3-D image, showing a root-mean-square roughness of 37.9 nm.

From the dual-electrodes measurement, the electrical conductivity of a protonated PANI layer is 13.2 S cm^{-1}, which is of the same order of magnitude as the earlier report in the literature [27]. It should be pointed out that the electrical conductivity of the PANI layer exceeds 0.20 S cm^{-1}, the conductivity of the Vulcan XC-72 activated carbon support. With subsequent hot-pressing of the catalyst layer on the PANI/N117, the PANI layer can enhance the electrical conductivity of the anode.

On the other hand, the proton conductivity of the membrane, σ, can be expressed as

$$\sigma = \frac{L}{R \times A}, \tag{3}$$

where R, L and A are the measured resistance, the membrane thickness and the membrane area, respectively, under the assumption that PANI is deposited only on the surface of the membrane and does not short-circuit the membrane. In the calculation of the methanol permeability, the gradient of the methanol concentration through the membrane is assumed to be linear and to follow the Fick law

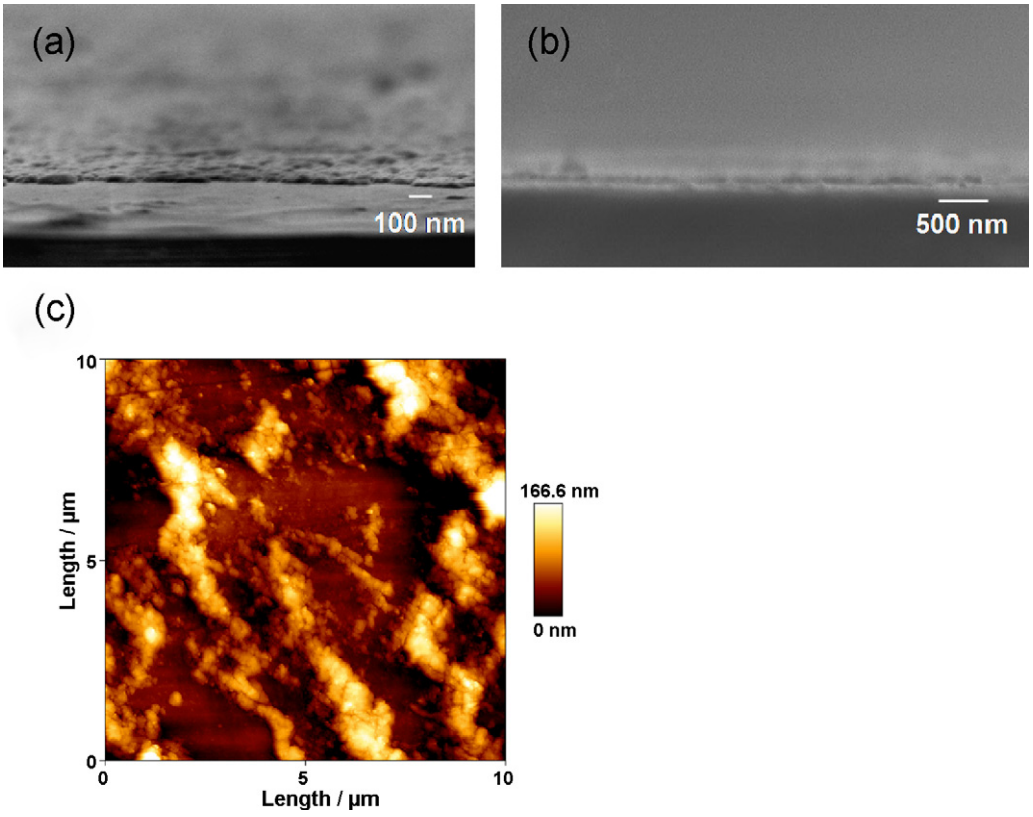

Fig. 3. The cross-sectional HRSEM images of the PANI deposited on (a) the silicon substrate and (b) the N117; the 3-D image of (c) the surface roughness of the PANI/N117 recorded by AFM.

Table 2
The proton conductivity and the methanol permeability of the specific membrane.

	N117	PANI/N117
Proton conductivity ($S\,cm^{-1}$)	0.0143	0.0099
Methanol permeability ($cm^2\,s^{-1}$)	2.83×10^{-6}	1.66×10^{-6}

[37],

$$\ln \frac{C_m - C_w}{C_{m,0} - C_w} = -\frac{DA}{lV}t, \quad (4)$$

where C_m is the transient methanol concentration of the methanol chamber, C_w is the transient methanol concentration of the deionized water chamber, $C_{m,0}$ is the initial methanol concentration of the methanol solution, D is the methanol permeability, and A, l and V are the cross-sectional area of membrane, the thickness of membrane and the volume of the sample solution, respectively. Table 2 presents the proton conductivity and the methanol permeability of the PANI/N117 composite membrane and of the N117 membrane thus obtained. The proton conductivity of the PANI/N117 is approximately 70% that of the N117 alone while the methanol permeability of the PANI/N117 is 59% that of N117. It clearly indicates that the PANI layer coated on the N117 membrane surface can act as a pore-filling agent to reduce the methanol permeability without significantly reducing the proton conductivity.

Fig. 4a and b depict the polarization curves of the PANI/N117-based and the N117-based MEAs, respectively, at different feeding methanol concentrations. The maximum power densities of the N117-based MEA were 85, 60, 55, 35 and 30 mW cm^{-2} at methanol solution concentrations of 1, 2, 4, 6 and 8 M, respectively, indicating that poorer performances at higher methanol concentrations. However, the maximum power densities of the PANI/N117-based MEA were 20, 40, 55, 70 and 53 mW cm^{-2} at methanol solution concentrations of 1, 2, 4, 6 and 8 M, respectively. The output power increases with increasing methanol concentration, to a maximum at 6 M methanol. Compared with the N117-based MEA, the PANI/N117-based MEAs is superior to the N117-based MEA at methanol concentrations above 4 M. Fig. 4 also compares the open circuit voltages (OCVs) of the two MEAs, and reveals that the OCV of the PANI/N117-based MEA has always exceeded that of the N117-based MEA. Based on the results of Qi and Kaufman [33] that the open circuit voltage is related to the activation of the electrocatalysts and the concentration of methanol at the cathode, the OCV results clearly indicate the reduction of the methanol crossover when using the PANI/N117-based MEA.

Fig. 5a and b plot the applied voltages as functions of the methanol-crossover current densities of the N117-based and the PANI/N117-based MEAs, respectively, operated at various methanol

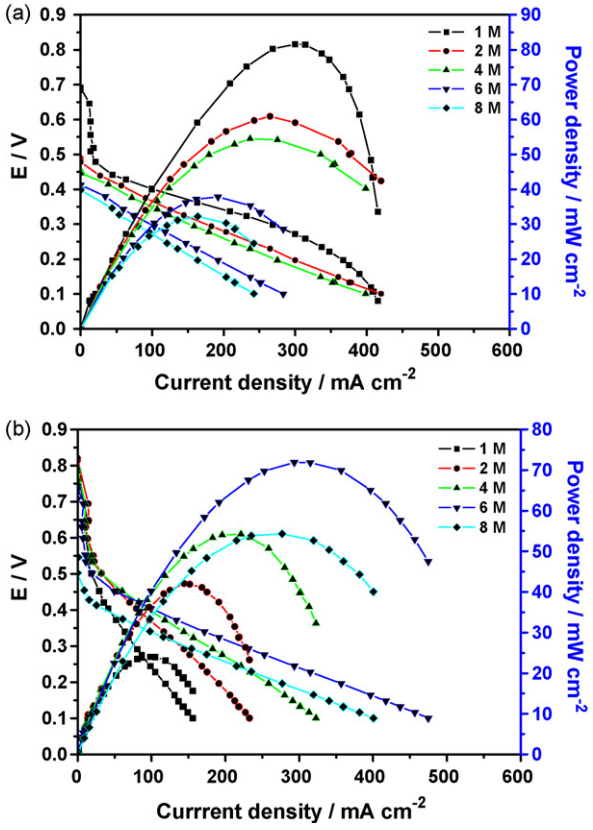

Fig. 4. The polarization curves of (a) N117-based MEA and (b) PANI/N117-based MEA operated at various methanol concentrations; the oxygen flow rate of 200 sccm, the methanol flow rate of 20 ml min^{-1} and the cell temperature of 60 °C.

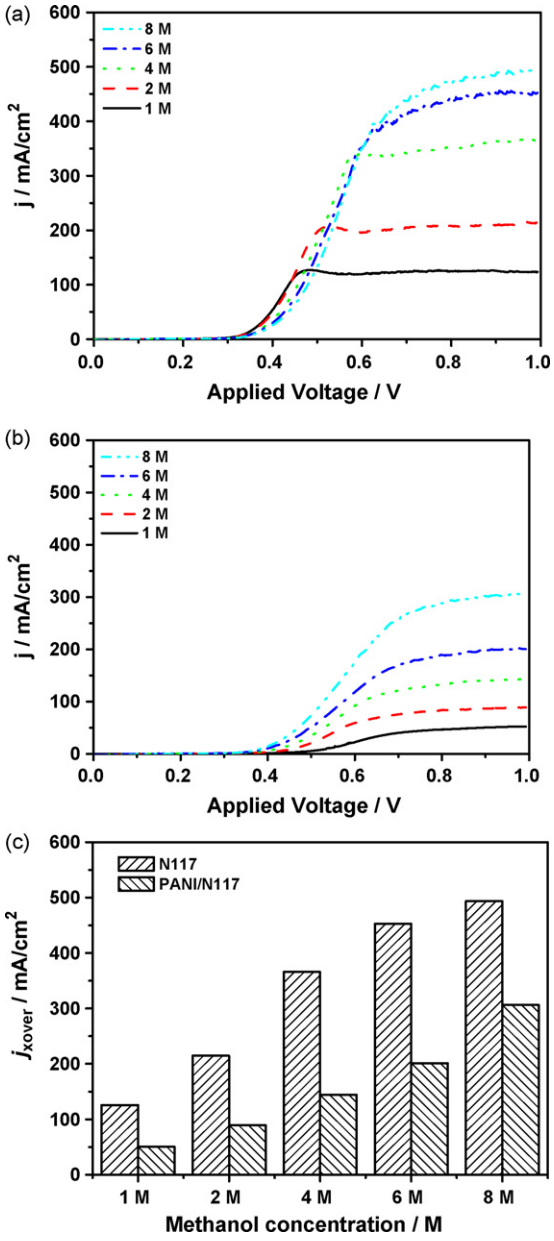

Fig. 5. The methanol-crossover current densities of (a) the N117-based MEA and (b) the PANI/N117-based MEAs operated at various methanol concentrations; (c) the methanol-crossover limiting current densities determined by the applied voltage of 1 V from (a) and (b).

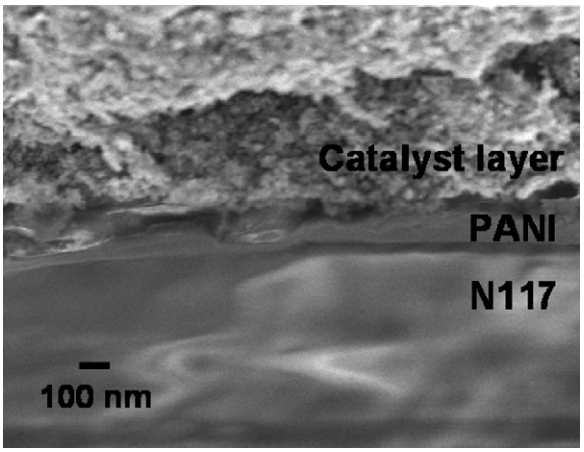

Fig. 6. The cross-sectional HRSEM image of the PANI/N117-based MEA.

concentrations. Figures demonstrate that all current densities almost reach a steady-state when a voltage over 0.9 V is applied. Accordingly, the methanol-crossover limiting current densities are determined by the applied voltage of 1 V (Fig. 5c). According to Fig. 5c, the methanol-crossover limiting currents of the PANI/N117-based MEA are approximately 60.0, 58.4, 60.6, 55.5 and 37.9% those of the N117-based MEA at 1, 2, 4, 6, and 8 M methanol solutions, respectively. These values are consistent with our earlier statements that the PANI layer substantially reduces methanol crossover in the MEA. Fig. 6 shows the cross-sectional HRSEM image of the PANI/N117-based MEA to present the morphology of a PANI layer that is sandwiched in the MEA. The image reveals that the PANI layer is compatible with the N117 and the catalyst layer with a thickness of about 100 nm after the hot-pressing process.

In order to understand the features of membranes operated at the various methanol concentrations, the resistances of N117 and PANI/N117 were determined by the high-frequency-impedance measurements during the DMFC operations. Fig. 7a shows that the resistances of N117 are consistently ca. 0.75 $\Omega\,cm^2$ at the various methanol concentrations. However, the resistance of PANI/N117 is ca. 2.0 $\Omega\,cm^2$ at 1 M methanol solution (not shown in Fig. 7b), and then it is reduced to ca. 1.2 $\Omega\,cm^2$ at the high methanol concentrations, as shown in Fig. 7b. The feature suggests that the conductivity of PANI/N117 is increased due to the elevated methanol concentration. Some previous works have suggested that the methanol hydrogen bonds, via one of the lone pairs on its oxygen atom, bond directly to the PANI, and therefore the effect of the hydrogen bonding is to push the polymer chains apart, uncoiling them, resulting in the increase of their conductivity [38,39].

Comparative to the N117-based MEA, the PANI/N117-based MEA has better performance at high methanol concentrations. The PANI layer located on the surface of N117 not only enhances the electrical conductivity and interaction of the catalysts but also reduces the methanol diffusion through the N117. Some PANI participants occupy parts of N117 structure, and therefore the interaction of aniline with the sulfonic acid group of Nafion results in blocking of the proton transport and the methanol diffusion.

When the DMFC is operated at elevated methanol concentration, the increase in the methanol-crossover overpotential occurs. Comparative to the N117-based MEA, the PANI/N117-based MEA has better performance at higher methanol concentration, indicating that the methanol-crossover overpotential does not limit the PANI/N117-based MEA at elevated methanol concentration. Besides, the impedance measurement shows that the PANI/N117-based MEA has a lower resistance at a higher methanol concentration, and therefore the PANI/N117-based MEA is favorable for the DMFC operation at the elevated methanol concentrations.

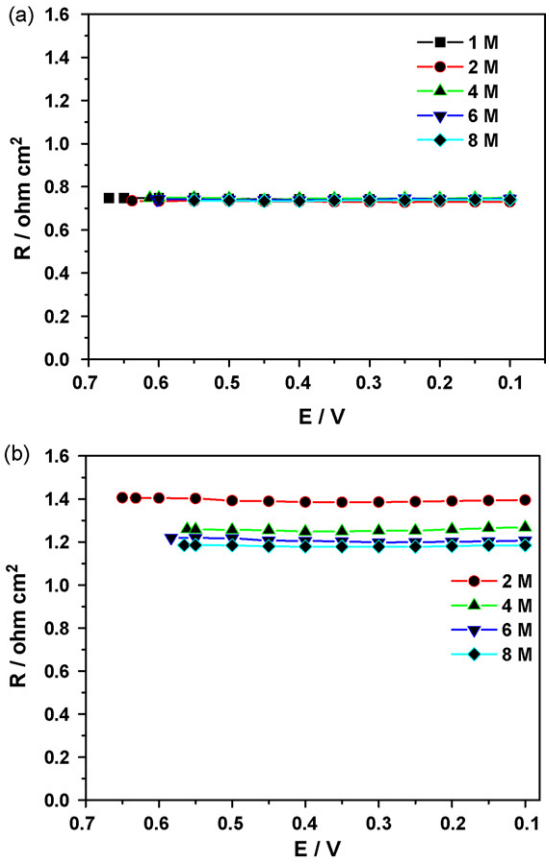

Fig. 7. The membrane resistances of (a) the N117-based MEA and (b) the PANI/N117-based MEA at various methanol concentrations under DMFC operations.

When the PANI/N117-based MEA is operated above 6 M methanol solution, the methanol-crossover overpotential is supposed to dominate the performance, leading to the decrease of output power.

4. Conclusions

This work demonstrates the performance of the PANI/N117-based MEA, in which the PANI is deposited on the Nafion 117 as a methanol-blocking layer. While the output power of the conventional N117-based MEA is reduced by increasing the methanol concentration due to methanol crossover, the output power of the PANI/N117-based MEA is increased at higher methanol concentration with a maximum output at 6 M methanol. This clearly demonstrates that the PANI/N117-based MEA effectively reduces methanol crossover and performs well when operated at elevated methanol concentrations, which is highly desirable for the small-scale DMFC in portable devices and microelectromechanical systems.

Acknowledgements

The authors would like to thank the National Science Council, and the Ministry of Education in Taiwan, the Grant Agency of the Academy of Sciences of the Czech Republic (A4050313), and the Asian Office of Aerospace Research and Development under AFOSR for financial support.

References

[1] A. Heinzel, V.M. Barragan, J. Power Sources 84 (1999) 70–74.
[2] J. Zhang (Ed.), PEM Fuel Cell Electrocatalysts and Catalyst Layers—Fundamentals and Applications, Springer, 2008.

[3] V. Neburchilov, J. Martin, H. Wang, J. Zhang, J. Power Sources 169 (2007) 221–238.
[4] C.-H. Wang, H.-Y. Du, Y.-T. Tsai, C.-P. Chen, C.-J. Huang, L.C. Chen, K.H. Chen, H.-C. Shih, J. Power Sources 171 (2007) 55–62.
[5] T. Schultz, S. Zhou, K. Sundmacher, Chem. Eng. Technol. 24 (2001) 1223–1233.
[6] T. Schaffer, T. Tschinder, V. Hacker, J.O. Besenhard, J. Power Sources 153 (2006) 210–216.
[7] Y.-M. Kim, K.-W. Park, J.-H. Choi, I.-S. Park, Y.-E. Sung, Electrochem. Commun. 5 (2003) 571–574.
[8] W.C. Choi, J.D. Kim, S.I. Woo, J. Power Sources 96 (2001) 411–414.
[9] P. Dimitrova, K.A. Friedrich, B. Vogt, U. Stimming, J. Electroanal. Chem. 532 (2002) 215–225.
[10] Y.-I. Park, J.-D. Kim, M. Nagai, J. Mater. Sci. Lett. 19 (2000) 1621–1623.
[11] S.P. Nunes, B. Ruffmann, E. Rikowski, S. Vetter, K. Richau, J. Membr. Sci. 203 (2002) 215–225.
[12] J.S. Wainright, J.-T. Wang, D. Weng, R.F. Savinell, M. Litt, J. Electrochem. Soc. 142 (1995) L121–L123.
[13] Y. Woo, S.Y. Oh, Y.S. Kang, B. Jung, J. Membr. Sci. 220 (2003) 31–45.
[14] V. Tricoli, F. Nannetti, Electrochim. Acta 48 (2003) 2625–2633.
[15] M. Matsuguchi, H. Takahashi, J. Membr. Sci. 281 (2006) 707–715.
[16] B. Smitha, S. Sridhar, A.A. Khan, J. Membr. Sci. 259 (2005) 10–26.
[17] S. Joseph, J.C. McClure, R. Chianelli, P. Pich, P.J. Sebastian, Int. J. Hydrogen Energy 30 (2005) 1339–1344.
[18] H. Gharibi, M. Zhiani, R.A. Mirzaie, M. Kheirmand, A.A. Entezami, K. Kakaei, M. Javaheri, J. Power Sources 157 (2006) 703–708.
[19] J.-H. Choi, Y.-M. Kim, J.-S. Lee, K.-Y. Cho, H.-Y. Jung, J.-K. Park, I.-S. Park, Y.-E. Sung, Solid State Ionics 176 (2005) 3031–3034.
[20] X.F. Li, D. Chen, D. Xua, C. Zhao, Z. Wang, H. Lu, H. Na, J. Membr. Sci. 275 (2006) 134–140.
[21] T. Shimizu, T. Naruhashi, T. Momma, T. Osaka, Electrochemistry 70 (2002) 991–993.
[22] T.K. Na, H.S. Kim, J.H. Park, T.H. Lee, 205th Meeting of the Electrochemical Society, MA 2004-01, 2004, p. 349.
[23] Y. Kang, D.W. Kim, J. Kwon, S. Park, J.-H. Choi, Y.-E. Sung, 206th Meeting of the Electrochemical Society, MA 2004-02, 2004, p. 2033.
[24] B.G. Choi, H. Park, H.S. Im, Y.J. Kim, W.H. Hong, J. Membr. Sci. 324 (2008) 102–110.
[25] Q.M. Huang, Q.L. Zhang, H.L. Huang, W.S. Li, Y.J. Huang, J.L. Luo, J. Power Sources 184 (2008) 338–343.
[26] C.-Y. Chen, J.I. Garnica-Rodriguez, M.C. Duke, R.F.D. Costa, A.L. Dicks, J.C.D. da Costa, J. Power Sources 166 (2007) 324–330.
[27] J. Stejskal, R.G. Gilbert, Pure Appl. Chem. 74 (2002) 857–867.
[28] K.-H. Lubert, L. Dunsch, Electrochim. Acta 43 (1998) 813–822.
[29] S.P. Armes, J.F. Miller, Synth. Met. 22 (1988) 385–393.
[30] J. Stejskal, P. Kratochvíl, M. Helmstedt, Langmuir 12 (1996) 3389–3392.
[31] J. Stejskal, I. Sapurina, Pure Appl. Chem. 77 (2005) 815–826.
[32] A. Riede, M. Helmstedt, I. Sapurina, J. Stejskal, J. Colloid Interface Sci. 248 (2002) 413–418.
[33] Z.G. Qi, A. Kaufman, J. Power Sources 110 (2002) 177–185.
[34] X. Ren, T.E. Springer, S. Gottesfeld, J. Electrochem. Soc. 147 (2000) 92–98.
[35] C. Barthet, M. Guglielmi, J. Electroanal. Chem. 388 (1995) 35–44.
[36] C. Barthet, M. Guglielmi, Electrochim. Acta 41 (1996) 2791–2798.
[37] K. Lee, J.-D. Nam, J. Power Sources 157 (2006) 201–206.
[38] X. Li, E.P.L. Roberts, S.M. Holmes, J. Power Sources 154 (2006) 115–123.
[39] A.A. Kulikovsky, Electrochem. Commun. 5 (2003) 1030–1036.